VERSITA

Acta Geophysica
vol. 60, no. 3, Jun. 2012, pp. 809-832
DOI: 10.2478/s11600-012-0006-z

Scaling Features of Ambient Noise at Different Levels of Local Seismic Activity: A Case Study for the Oni Seismic Station

Teimuraz MATCHARASHVILI[1,2], Tamaz CHELIDZE[1], Zurab JAVAKHISHVILI[2], Nato JORJIASHVILI[2], and Natalia ZHUKOVA[1]

[1]M. Nodia Institute of Geophysics, Tbilisi, Georgia
e-mail: Matcharashvili@gtu.ge (corresponding author)

[2]Ilia State University, Tbilisi, Georgia

Abstract

Investigation of dynamical features of ambient seismic noise is one of the important scientific and practical research challenges. We investigated scaling features of the ambient noises at the Oni seismic station, Georgia, using detrended fluctuation analysis method. Data from this seismic station, located in the epicentral zone of Oni *M*6.0, 2009, earthquake, were selected to include time periods with different levels of local seismic activity.

It was shown that the investigated ambient noise is persistent long-range correlated at calm seismic conditions in the absence of earthquakes. Fluctuation features of the analyzed ambient noises were affected by local earthquakes, while remote seismic activity caused just slight quantitative changes. Processes related to the preparation of a strong local earthquake may cause quantifiable changes in fluctuation features of ambient noises. Fluctuation features of seismic noise for periods of increased local seismic activity cease to be long-range correlated and appear to become a complicated mixture of random and correlated behaviours.

Key words: ambient noise, earthquake, dynamics, scaling.

1. INTRODUCTION

Earthquakes (EQs) are regarded as one of the most dramatic phenomena occurring in nature, causing enormous human and economic loses. A multitude of underground events and fluctuations of the Earth's surface occur annually as a result of complex spatio-temporal phenomena related to the convective motion in the mantle, provoking relative motion of the faults bordering the tectonic plates. This leads to fast emission of energy propagating over long distances in the form of elastic seismic waves (Kanamori and Brodsky 2001). Thousands of seismic waves are worldwide detected by seismographs in the form of vibrations of the Earth's surface and have been collected in seismic data bases.

At the same time, seismic waves are not the only cause for the Earth surface vibrations. Many other factors, ranging from atmospheric pressure variation and ocean waves to human activity, always contribute to the vibrations of the Earth ground (Webb 1998, Yulmetyev *et al*. 2001, SESAME 2004, Correig *et al*. 2007). These vibrations − microseisms or microtremors − representing superposition of waves of different origin are often collectively named the ambient noises.

Because of their diverse origin and complicated spatio-temporal features, the Earth surface vibrations or ambient noise, represent random-like high-dimensional dynamical processes (Yulmetyev *et al.* 2001, 2003, Padhy 2004, Correig *et al*. 2007, Lyubushin 2010, Sobolev *et al.* 2010). Such complicated processes are normally characterized by uniform spectral features and dynamical structure, which are extremely difficult to be quantified.

On the other hand, the seismic signals contributing to the ambient noise are regarded as having more regular dynamical structure comparing to random noise (Padhy 2004, Tabar *et al*. 2006, Manshour *et al*. 2009). This looks quite logical in the light of, as has been established in the last decades, the presence of nonrandom, though high-dimensional dynamical structure in the seismic process – the source of seismic signals (see *e.g.*, Goltz 1997, Lapenna *et al.* 1998, Rundle *et al.* 2000, Matcharashvili *et al*. 2000, Chelidze and Matcharashvili 2007, Matcharashvili and Chelidze 2010). Physically, the presence of nonrandom dynamical structure in the earthquake (EQ) generation processes, and seismic waves accordingly, is related to the processes accompanying stress accumulation and the breakdown of a disordered solid together with concomitant stick-slip movement. Generally speaking, these complex processes, involving cascades of transitions (changes) in wide spatial, temporal and energetic scales are, or can be, in principle detectable. Some of these transitions − precursory changes − preceding or accompanying breakdown and stick-slip movement in disordered solid rocks, have already been observed both at the laboratory and geophysical scales (Kapiris

et al. 2003, Telesca and Lapenna 2006, Karamanos *et al.* 2006, Chelidze *et al.* 2006, Tabar *et al*. 2006, Manshour *et al.* 2009). It is also understandable that, because of the complexity of seismic process, such changes might be of different forms, related to variations in mechanical, chemical, hydrological, electromagnetic, and other processes in the seismic source or peculiarities of wave propagation in rocks, *e.g.*, acoustic or electromagnetic emissions (Karamanos *et al*. 2006, Tabar *et al*. 2006).

At the same time, it should be stressed here that opinions about the researches on the marker changes which may have earthquake predictive value are still controversial. It is not clear what changes, in which characteristics, and to what degree, can be regarded as precursors, or what may be the length of the spatial and time scales over which different precursory anomalous changes may occur and accumulate. At present, there are many pro and contra arguments in these precursory-related discussions. There are also contradictions between supporters of precursory phenomena. Some authors assume that precursory patterns develop at short spatial distances, within few days to weeks before the main shock from the impending large earthquakes, while others claim that precursory anomalies may occur up to decades before it at distances much longer than the length of the main shock rupture (Scholz 1990, Keilis-Borok and Soloviev 2003, Tabar *et al.* 2006).

Notwithstanding all these difficulties, changes in the dynamical features of ambient surface noise, caused by processes related to the earthquake preparation, are by many authors assumed to be quantifiable and are regarded among possible precursors (Padhy 2004, Tabar *et al.* 2006, Sobolev and Lyubushin 2006, Manshour *et al*. 2009, 2010). Moreover, in the context of possible dynamical changes it was suggested that as the final failure in the disordered media is approached, the underlying complexity manifests itself in specific linkages between space and time features. This in turn may lead to producing detectable (precursory) patterns on many scales and the emergence of fractal structures in different accompanying process (Karamanos *et al*. 2006).

In general, the present level of dynamical data analysis enables these changes in dynamical structure of the Earth surface vibrations to be assessed qualitatively and quantitatively. Indeed, in the last years, a lot of interdisciplinary research works have been devoted to the complexity of seismic noises, analysis of their fractal, power law, long memory and many other statistical and dynamical features in order to detect and describe the spatial, temporal and energetic scaling properties of the processes related to earthquake preparation (Yulmetyev *et al.* 2001, Padhy 2004, Tabar *et al*. 2006, Correig *et al.* 2007, Caserta *et al*. 2007).

In the present research, we focus on the fluctuation features of the ambient seismic noise time series using similar concepts. The main goal of this

research was to carry out comparative analysis of scaling features of ambient noise time series in the time periods of increased as well as relatively low local seismic activity on the example of seismic data recorded at Oni seismic station in Georgia. The advantage of specified location was that the Oni station is situated close to the last strongest Caucasian earthquake of *M*6.0, which occurred in September 2009.

The targeted problem on fluctuation features of local seismic noise is of general interest and has a great scientific significance, being related to the recognition of changes in apparently similar signals with different physical origins. The recognition of changes caused by an arrival of seismic signals in the background random noise is of prime importance from scientific and practical points of views. Such analyses of seismic data are often the subject of vivid interests for different purposes, including earthquake forecasting, and numerous methods of data analysis are used (Yulmetyev *et al.* 2001, 2003, Caserta *et al.* 2007).

2. THE DATA USED AND METHODS OF ANALYSIS

The data used in this study are digital seismograms recorded by broad-band permanent station located in Great Caucasus mountains near the town Oni (42.5905°N, 43.4525°E), Georgia (Fig. 1). We investigated all three components of vibrations of the Earth's surface, but mainly focused on time

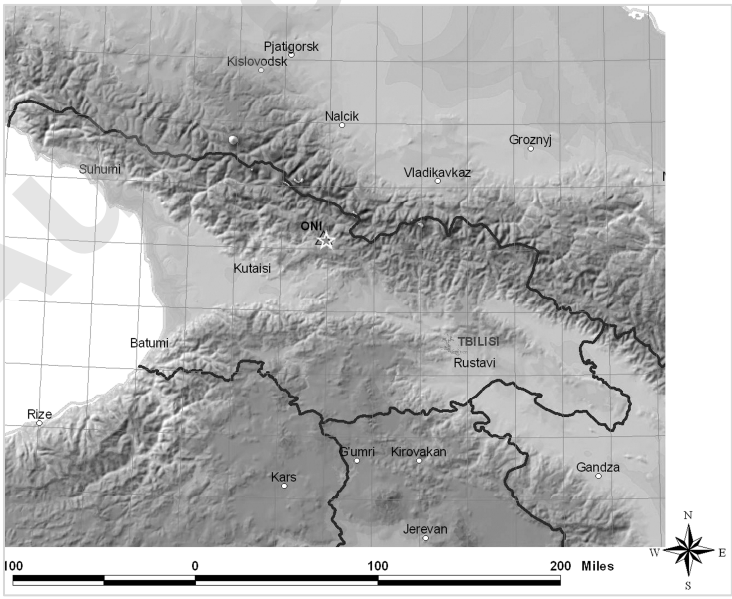

Fig. 1. Map of location of Oni seismic station. By the star, the epicenter of Racha *M*6.0 earthquake is shown.

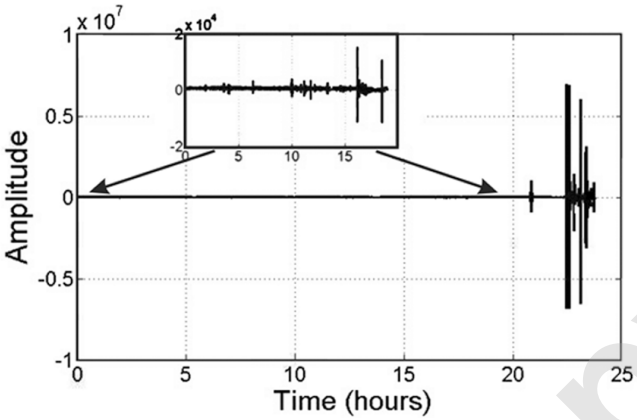

Fig. 2. The ambient noise data record including waveforms of the *M*6.0 Racha earthquake.

series of the Earth's vertical velocity, V_z (see a typical four-day recording in Fig. 2). The data were recorded at a sampling frequency of 100 Hz with a dynamic range over 140 dB. The station has a flat velocity response from 0.01 to 100 Hz frequency band. The seismograms are corrected for instrument response before the analysis, so as to get the ground velocity. The seismic station Oni is part of seismic network operated by the Ilia State University, Seismic Monitoring Centre of Georgia.

In order to compare scaling characteristics of ambient noise data sets at different levels of local seismic activity, we selected datasets for different time periods. Namely, the four-day recordings preceding the Racha *M*6.0 earthquake (22:41:35 UTC on 7 September 2009; 42.5727°N, 43.4825°E), the epicenter of which was located at a distance of 4 km from the Oni station, have been investigated at first.

In these recordings, waveforms arriving from two remote earthquakes are visible. Namely, the *M*4.9 EQ occurred in Afghanistan (09:01:53 UTC on 7 September 2009; 36.45°N, 70.73°E) and the *M*6.2 EQ occurred in Indonesia (16:12:22 UTC on 7 September 2009; 10.20°N, 110.63°E). Besides, two foreshocks of the Racha earthquake occurred during this four-day period: *M*1.6 (14:06:35 UTC on 3 September 2009; 42.5414°N, 43.5282°E) and *M*2.1 (14:17:31 UTC on 3 September 2009; 42.5508°N, 43.528°E). Seismic waveforms from all these events are involved in the analyzed time series. So, ambient fluctuations at Oni station in the considered case were affected by strong and weaker local, as well as by remote seismic activities. The next series of analysis were accomplished on seismic record data sets for the time period in March 2011, when no local seismic activity was detected. At the end of this period, arrivals of waveforms from Japan *M*9.0

earthquake (05:46:24 UTC on 11 March 2011; 38.322°N, 142.369°E) were recorded by the Oni station. Additionally, seismic records were considered from 23:59 UTC on 21 January 2009 to 19:00 UTC on 22 January 2009, when no local and remote seismic activity was detected by broad-band Oni station. In addition, we selected the period from 18:00 UTC on 20 January 2011 to 16:00 UTC on 21 January 2011. This period can also be regard as locally calm because no seismic activity was detected by broad-band Oni station and epicenter of Vani (Georgia) *M*5.3 earthquake, located about 100 km from the station (09:17:49 UTC; 41.9458°N, 42.6935°E), occurred 33 h before this time period. Other period considered was from 00:00 to 18:59 UTC on 30 October 2010, when a slight local seismic activity was detected (series of *M*0.7-*M*1.6 events occurred in 10 km area around the Oni station) and also waveforms that arrived from *M*5.2 earthquake, which occurred in Japan (19:06:19 UTC on 30 October 2010; 34.38°N, 141.33°E).

In general, complex systems time series, like ambient noise, exhibit fluctuations on a wide range of time scales, which is often accompanied by the broad amplitude and frequencies distributions. Such fluctuations usually follow scaling laws, which allow characterization of the data and the generating complex system by fractal (or multifractal) scaling exponents. The know- ledge of these scaling exponents is very important because they provide unique information on systems' behavior and may serve as characteristic fingerprints for comparison with other systems and models.

In this research, in order to quantify scaling features of ambient noise, detrended fluctuation analysis (DFA) method has been used (Peng *et al.* 1993a, b; 1995). We selected DFA in order to quantify long-range time-correlations in the investigated ambient noise data sets. Usually DFA is conceived as a method for detrending local variability in a sequence of events, which provides insight into long-term variation features in the complex data sets. This scaling analysis technique provides a simple quantitative parameter (DFA scaling exponent) representing the correlation properties of a time series. As already mentioned, the very important practical advantage of DFA over many other scaling techniques is that it enables the detection of long-range correlations embedded in the time series. Moreover, DFA helps to avoid the spurious detection of apparent long-range correlations that are an artifact of non-stationarity.

In practice, the DFA method consists of three steps (Peng *et al.* 1993a, b). First, the initial time series $x(k)$ (of length N) is integrated and "profile" $Y(i)$ is determined. After this, the resulting series $Y(i)$ is divided into boxes of size n. In each box of length n, local trend, $Y_n(i)$, is calculated. Next, the line points are subtracted from the integrated series $Y(i)$ in each box. The root mean square fluctuation of the integrated and detrended series is calculated as

$$F(n) = \sqrt{\frac{1}{N}\sum_{i=1}^{N}\left[Y(i) - Y_n(i)\right]^2} \ .$$

This process is repeated for different scales (box sizes) to obtain a power law behavior between $F(n)$ and n. When the signal follows the scaling law, a power law behavior for the function $F(n)$ is observed:

$$F(n) \sim n^{\alpha} \ .$$

The scaling exponent α gives information about the long-range power law correlation properties of the signal (Peng *et al.* 1993a, b; 1995, Ivanov *et al.* 2002, Rodriguez *et al.* 2007). Specifically, the scaling exponent $\alpha = 0.5$ corresponds to white noise (noncorrelated signal); when $\alpha < 0.5$, the correlation in the signal is anti-persistent; if $\alpha > 0.5$, the correlation in the signal is persistent. The value $\alpha = 1$ means uniform power law behavior of $1/f$ noise. The value $\alpha = 1.5$, indicating uncorrelated behavior, represents a random-walk type process of Brownian motion. The value $\alpha > 1.5$ corresponds to persistent long-range correlations that may be related to both stochastic and deterministic correlations, and $\alpha < 1.5$ corresponds to anticorrelated behavior.

It may often happen that the correlations of recorded data do not follow the same scaling law for all considered n time scales. In such cases, the function $F(n)$ displays different power-law behaviors and in the double logarithmic plots of the DFA fluctuation function, one or more crossovers between different scaling regimes are observed. These crossover (time) scales separate regimes with different scaling exponents (Peng *et al.* 1995, Ivanov *et al.* 2002, Kantelhardt *et al*. 2002). In practice, the crossover region is defined by the values of n where the function $F(n)$ changes its behavior.

Quantification of the fractal properties through calculation of scaling exponent by the above methods is often used to describe features of complex systems behavior. In the frame of this research, we calculated DFA scaling exponent for consecutive non-overlapping sliding windows of different length. By this method, it was established that the time window of 2 min duration is the most appropriate one, enabling to cover the scaling region of fluctuation curve, indicating at the same time the presence of periodic trends at larger time scales.

3. RESULTS AND DISCUSSION

In Figure 3, an example of a power spectrum of seismic noise data recorded at the Oni station is presented. It is similar to the power spectrums for data sets from other broad-band seismic stations worldwide, with a typical

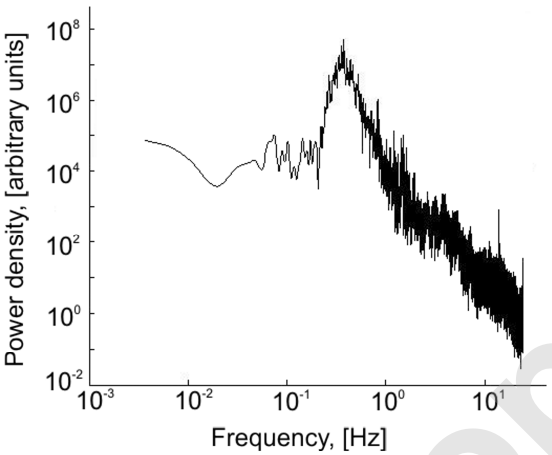

Fig. 3. Typical power spectrum of seismic noise recorded at the Oni station.

location of the largest spectral peak, sometimes regarded as an observational invariant for such data (Correig *et al.* 2007, Ryabov *et al.* 2003).

As already mentioned, we selected data sets recorded at Oni seismic station because it is located very close (4 km) to the epicenter of strong *M*6.0 earthquake that occurred on 7 September 2009 (22:41:35 UTC; 42.5727°N, 43.4825°E). Besides, two foreshocks of the *M*6.0 main shock also occurred within 10-km distance from the Oni station. An analysis of such good-quality data sets from a rural place with low anthropic influences, recorded almost in the centre of the critical zone of a strong earthquake, looked very interesting from the point of view of detecting changes in the ambient noise fluctuation features, which can possibly be related to the local earthquake preparation process.

The total length of the ambient noise data series used in our research, recorded for time periods of different duration (1 to 4 days), were in the range from about 10 to 35 million. We started from the investigation of correlation characteristics of ambient noise data sets by the DFA, a method enabling to avoid effects of nonstationarities in data sets. As already mentioned, DFA is often successfully used for data sets of different origin in different fields, including geophysics and seismology (*e.g.*, Peng *et al.* 1993a, b; 1995, Telesca *et al*. 2005, 2008, Bunde *et al.* 2002, *etc*.). It was most attractive for the purpose of our research that the DFA method enables identifying different states of the dynamical system according to its different scaling behaviors (Peng *et al.* 1995, Hu *et al*. 2001). Thus, it may help to find out whether quantifiable changes in local Earth surface vibrations have occurred prior to the strong earthquake, which can be regarded as related to local seismic activity.

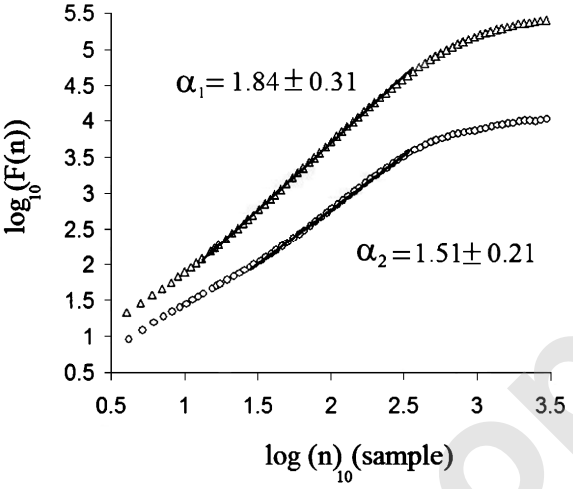

Fig. 4. Averaged DFA fluctuation curves obtained for *Z*-components of seismic noise records at the Oni station. The lower curve corresponds to the period covering 72 h before and 20 h after the 2009 Racha *M*6.0 EQ, including foreshocks, as well as the arrival of waveforms from remote events and aftershocks. The upper curve corresponds to periods of 48 h before the arrival of waveforms from remote Japan *M*9.0 EQ and 10 h after. Curves are shifted along the *y* axis for clarity.

In Figure 4, DFA plot of averaged $\log F(n)$ *versus* $\log n$ relation calculated for ambient noise data recorded at the Oni station is presented. Calculations have been carried out for consecutive 12 000 sample data length non-overlapping (2 min) windows of ambient seismic noise of the *Z*-component records. The lower curve corresponds to time period of increased local seismic activity around the Oni station and includes seismic waveforms from foreshock, main shock, and aftershocks of the Racha *M*6.0 earthquake as well as wavetrains from remote Afghanistan *M*4.9 and Indonesia *M*6.2 earthquakes (see the methods section). The upper curve corresponds to time period of low local seismic activity and includes wavetrains from devastating *M*9.0 earthquake that occurred in Japan in March 2011. According to Fig. 4, averaged $F(n)$ *versus* n relation, for both time series considered, looks generally similar, though slopes of scaling linear parts of curves are different. Also, it is noticeable that the linear scaling part of fluctuation curves, indicating the power law $F(n)$ *versus* n relation, is longer for data sets recorded at a seismically quiet period around the Oni station in March 2011 comparing to fluctuation curve of seismic noise in September 2009, when the *M*6.0 earthquake occurred. We also see in Fig. 4 the crossover points separating regimes of ambient noise vibrations with different scaling characteristics. Crossover points' locations are not coinciding for these data sets because of

the above-mentioned different lengths of fluctuation function scaling regions. At low frequencies, the crossover time scales are about 3 s in both cases. In the high frequency range, the crossover time scale is 0.3 s for the period when the 2009 Oni *M*6.0 earthquake occurred. At the same time, for three-day long data set recorded in March 2011, a crossover at higher frequencies is hardly identifiable and seems to be at about 0.1 s.

Next, in order not to be restricted by the results of averaged slopes and to better compare scaling properties of complicated ambient noise data sets for certain time periods, we performed additional distributional analysis of DFA scaling exponents. Specifically, for each 2 min windows, a scaling region of $\log F(n)$ *versus* n relation was identified and the slope was calculated. In Figure 5, histograms of these scaling exponents obtained for consecutive windows of the above-mentioned ambient noise data recorded in September 2009 (involving signal from the Racha *M*6.0 earthquake as well as its foreshocks and aftershocks) and in March 2011 (involving wavetrains from the Japan *M*9.0 earthquake) are presented. On the left side of Fig. 5, histograms of scaling exponents calculated for the same time series after shuffling procedure are presented. We see that more than 95% of scaling exponent values for both shuffled data sets are concentrated close to 0.5, corresponding to white noise (the significance of difference between the scaling exponents for original and shuffled data sets was quantified by the method described in

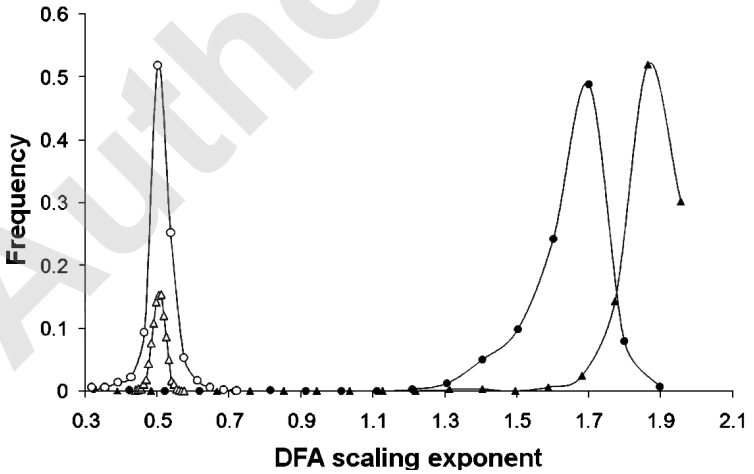

Fig. 5. The histograms of the scaling exponents calculated for consecutive windows of 12 000 sample of seismic noise *Z*-components data sets recorded at the Oni station. Dark circles correspond to 2836 windows involving the periods prior to the Racha *M*6.0 EQ, dark triangles correspond to 2100 windows in March 2011 involving the period before arrival of seismic waves from the Japan *M*9.0 EQ, open circles and triangles correspond to shuffled data sets.

Theiler *et al.* (1992). Contrary to this, original time series, by their DFA scaling exponents, are always much different from the white noise behavior (histograms on the right side of Fig. 5). These histograms indicate important differences in the fluctuation properties of the Earth surface vibration for the two time periods considered.

Results presented in Fig. 5 show that ambient seismic noise at increased local seismic activity comprises a multitude of processes of diverse dynamics, from uniform power law behavior of $1/f$ type ($\alpha = 1$) to long-range correlations; the latter one may be of stochastic fractional Brownian-motion type or even of deterministic nature ($\alpha > 1.5$). We see that at least 25% of DFA scaling exponent values calculated for time period before and after the strong local Racha earthquake occurrence indicate closeness to Brownian-motion type processes ($\alpha = 1.5$) and not less than 15% show anticorrelated behavior (dark circles in Fig. 5). At the same time, data recorded at a locally quiet period, before and after the arrival of seismic waves from the remote Japan *M*9.0 earthquake, always reveal a significant shift to the larger scaling exponents (up to $\alpha = 1.91$) indicating persistent long range correlation. It is worth to point out that in the last case the Brownian-motion type behavior was never observed and more than 98% of calculated DFA scaling exponents exceeded the value of 1.5.

These different kinds of fluctuation characteristics, with respect to scaling behavior, demonstrate different stochastic structures in ambient noise data sets at different levels of local seismic activity.

We point out again that all the results presented above were obtained for data sets which included waves of different local as well as remote origin. In order to see how the fluctuation features of ambient noise *Z*-component data may be influenced by the different seismic waveforms, we undertook an analysis for the time windows when wavetrains of certain origin were detected at the Oni station. Specifically, we focused on time windows under the following conditions: (i) neither local earthquakes occurrence nor arrival of wavetrains from remote earthquakes have been registered, (ii) only arrivals of waveforms from remote earthquakes were detected, (iii) strong local *M*6.0 earthquake occurred, and (iv) its aftershocks occurred.

Results of this analysis are presented in Fig. 6. In the lowest curve, results of calculations for the period prior to the Racha *M*6.0 earthquake are shown. Specifically, about 1700 windows of 12 000 data (2 min each), were selected so as to make the shape of fluctuation curves typical to the ones observed when no arrival of seismic waves have been detected at the Oni station. The fluctuation curve, averaged for all these time windows, shows clear crossovers at long and short time scales. Between these crossovers, we observe a linear scaling region. The presence of such a scaling part in this curve means that the ambient noise for considered periods revealed power

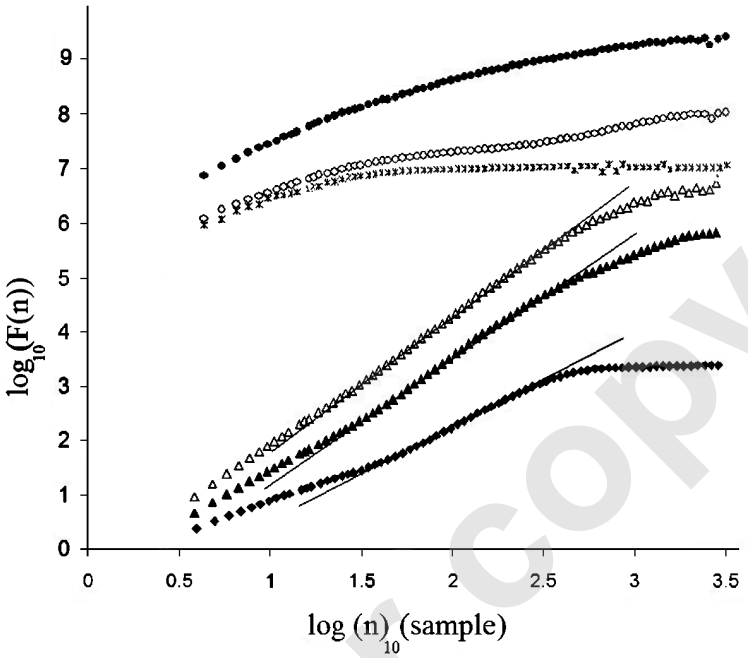

Fig. 6. Averaged DFA fluctuation curves obtained for the *Z*-component of seismic noise data at the Oni station calculated for consecutive non-overlapping 2-min windows. Diamonds – before the Oni *M*6.0 EQ for time windows with no local earthquakes and without arrival of remote waveforms; white and black triangles – for windows when the arrival of waveforms from remote earthquakes was detected; asterisks – for window when foreshocks of the Oni *M*6.0 event occurred; dark circles – for a window when the Oni *M*6.0 EQ occurred, and open circles when its aftershocks occurred. Curves are shifted along the *y* axis for clarity.

law behavior in the frequency range of about 0.3-3 Hz. For lower frequencies (longer time scales) we see breakdown of the power law scaling behavior, which can be observed in the systems when different quasi-periodic trends dominate (Hu *et al.* 2001, Alvarez-Ramirez *et al.* 2005). For small scales, at frequencies above 3-4 Hz, the linear relation is questionable, especially taking into consideration that for small scales of *n* the deviations from the scaling law are intrinsic to the usual DFA method (Peng *et al*. 1993a).

The next two curves in the upward direction in Fig. 6 correspond to time periods when seismic signals from remote events have arrived at Oni station prior to local *M*6.0 earthquake. We see that the arrival of wavetrains from remote events, *M*4.9 that occurred in Afghanistan and *M*6.2 in Indonesia (see the methods section for details), do not essentially change general fluctuation features of ambient noise around the Oni station. Indeed, as shown in Fig. 6,

the general shape of averaged DFA fluctuation curves of ambient seismic noise data, for the time windows when arrivals of wavetrains from the above-mentioned remote earthquakes have been detected, is similar to that for calm windows (the lowest curve in Fig. 6). At the same time, the frequency range and slope of scaling linear part seems to be larger in this case comparing to windows when no clear seismic waves were detected at the Oni station. Besides, the linear scaling region of fluctuation curve is longer and crossover points at small scales are not so clear for time periods of remote wavetrains arrival, but still detectable.

It is noticeable from Fig. 6 that a strong local seismic activity essentially alters the character of scaling features of ambient noise fluctuation. Indeed, fluctuation curves of seismic noise data for the time windows when the Oni *M*6.0 earthquake, as well as its foreshocks and aftershocks, occurred do not reveal credible scaling behavior. This means that contrary to remote seismic activity, the arrival of seismic waves from local earthquakes completely destroyed the fluctuation feature of ambient noise. This is quite logical taking into consideration the amount of strain energy released by an earthquake, which many times exceeds the energy sources of other components of seismic noise.

Thus we see in Figs. 4 and 6 (lower curves) that the shape of averaged fluctuation curves for the whole ambient noise data sets and for windows when no local or remote earthquakes have been detected are similar. In both cases, we observe crossovers and clear scaling regions. This can be understood as an indication that for the purpose of general consideration the use of whole data sets of ambient noise time series, without identification of the type of arrived signal, may be applicable.

At the same time, as it was already mentioned, the arrival of seismic waves, especially from a strong local event, can essentially affect fluctuation features of ambient noises (see Fig. 6). Apparently, both qualitative as well as quantitative changes in the earth surface vibrations occur for the certain time periods of seismic wave arrivals, which is revealed in changes of the shape as well as of the scaling features of fluctuation curves.

Therefore, in order to consider the dynamics of ambient noises and to be focused on the changes which can possibly be related to the local earthquake preparation, we intentionally eliminated from data sets those sections in which the arrival of remote or local seismic waveforms has been detected. Such compiled time series of ambient noise data, consisting of recordings at time periods when no arrival of seismic wavetrains at the Oni station was detected, have been considered prior to the Oni *M*6.0 earthquake occurrence in September 2009, as well as in March 2011, when wavetrains from Japan *M*9.0 earthquake arrived at the Oni station.

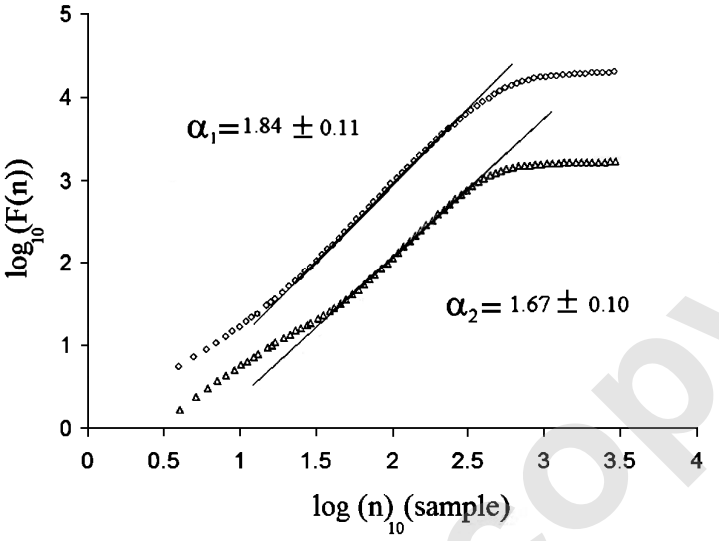

Fig. 7. Averaged DFA fluctuation curves of *Z*-components of seismic noise records at the Oni station when no local or remote seismic activity was observed. The lower curve corresponds to the period prior to the Racha *M*6.0 EQ (2009). The upper curve corresponds to the period before the arrival of waveforms from remote Japan *M*9.0 EQ. Curves are shifted along the *y* axis for clarity.

Results of analysis are shown in Fig. 7. We see two crossovers in $\log F(n)$ *versus* $\log n$ relation curves of both time series. Between these crossovers, time scales fluctuations of ambient noise always reveal long range correlations ($\alpha > 1.5$) for both data sets. Similar to the results for the whole data sets, results in Fig. 7 indicate different dynamical structures with respect to scaling behavior in the considered ambient noise data for seismically quiet and active time periods around the Oni station. Thus, the observed differences cannot be affected by the arrival of seismic wavetrains from local or remote earthquakes.

In addition to the above analysis of averaged fluctuation curves calculated for time periods when no local earthquakes and arrival of wavetrains from remote events were detected, we also calculated individual scaling exponents for consecutive 2-min time windows of locally quiet time periods. Results of calculation, presented in Fig. 8, show that the distribution range of scaling exponents is here somewhat narrower though in general similar to what we see for the whole data sets in Fig. 5. Differences mainly concern the lower and upper limits of scaling exponents' distribution range. It is interesting that the majority of encountered values of scaling exponents calculated for "calm" windows of seismically active and locally quiet periods become

closer in this case, comparing to what was found for the whole data sets. Anyway, we see from Fig. 8 that distribution functions of scaling exponents' values, for increased local seismic activity and for quiet periods, are still well distinguishable. By these results, ambient noises in calm seismic conditions indicate persistent correlated process ($\alpha > 1.5$), while at increased local seismic activity we observe the mixture of processes involving correlated, anticorrelated and uncorrelated behaviors ($1.2 < \alpha < 1.8$).

Thus, as we see in Fig. 8, the distribution of features of scaling exponents for the considered groups is different. Indeed, according to the Kolmogorov–Smirnov test, indicating the goodness of fit, the value of p for Gaussian distribution is 0.75 for ambient noise data prior to the Oni M6.0 earthquake and 0.9 for period before the arrival of wavetrains from the Japan M9.0 earthquake. This also provides an additional argument in favor of the opinion that the dynamics of seismic noises in the considered periods is different.

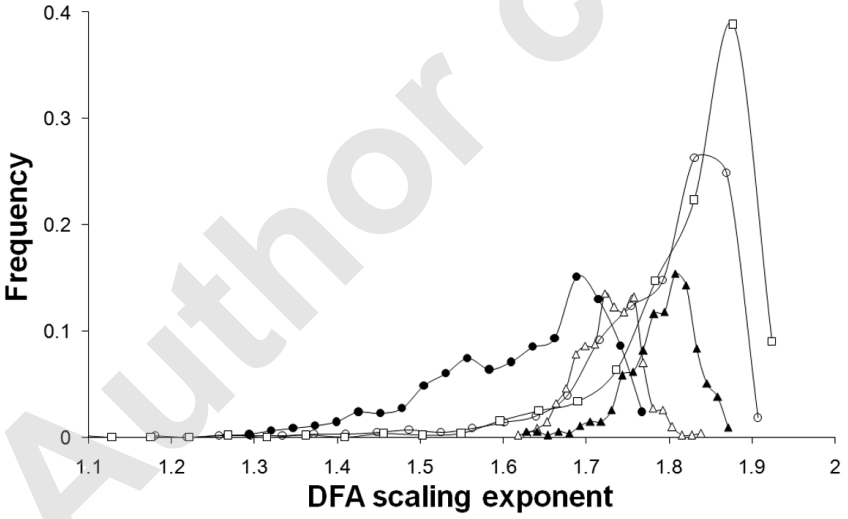

Fig. 8. The histograms of scaling exponents calculated for consecutive 12 000 sample data length windows of Z-components of seismic noise time series recorded at the Oni station for the periods regarded as seismically calm. Dark circles − time windows before the 2009 Racha M6.0 EQ, when no local activity or arrival of remote wavetrains were detected; dark triangles − time windows when before and after the arrival of wavetrains from the 2011 Japan M9.0 EQ no seismic activity was detected; open squares – period from 23:59 to 19:00 UTC on 22 January 2009, when no local activity or arrival of remote waves was detected; open circles – locally calm period from 00:00 UTC on 20 to 21 January 2011; open triangles – moderate seismic activity around the Oni station, period from 00:00 to 19:00 UTC on 30 October 2010.

It is of special importance to underline that this difference is not caused by the influence of seismic component of ambient noise (*i.e.*, by waves from local or remote earthquakes). Indeed, the result was practically the same when we selected quiet time windows only (when arrivals of seismic waves from local or remote earthquakes have not been detected at the Oni station).

Then, in order to exclude inaccuracies because of possible specificities of analyzed time periods, we tested our results for three additional periods. For this, we aimed to select one to several days long periods with local seismic activity as low as possible, and an additional period with moderate local seismic activity. Specifically, from the data sets of ambient noises recorded at Oni seismic station, a 20-hour period, from 00:00 to 19:00 UTC on 30 October 2010, was selected. As it was mentioned in the section on data and methods, the seismic activity around Oni station in this period slightly increased and, moreover, at the end of the selected time interval, arrivals of seismic waves from *M*5.2 earthquake that occurred in Japan were detected. The next time period was selected from 23:59 to 19:00 UTC on 21 January 2009. During this period and immediately before and after it, neither an increase of local seismic activity nor an arrival of seismic waves from remote earthquakes has been detected. A locally calm period was from 00:00 on 20 to 21 January 2011, 33 hours after the Vani (Georgia) *M*5.3 earthquake, whose epicenter was located about 100 km from the Oni station and thus the station was outside of critical zone ever detected for strong Caucasian earthquakes.

For these time periods, calculations of DFA scaling exponents, similar to those described above, have been carried out. In Figure 8, results of these calculations are presented in the form of histograms of DFA linear part scaling exponents. It can be seen that for time periods which can be regarded as locally quiet, because no seismic waveforms have been detected at Oni station, *e.g.*, in January 2009 and 2011 or March of 2011, the scaling exponent distribution looks similar to the one before the arrival of waves from Japan *M*9.0 earthquake, *i.e.*, for the time period which was locally quiet too. In these cases, the calculated values of ambient noise scaling exponents exceeded the value $\alpha = 1.5$, typical for a random walk, which indicates more persistent correlated behavior. On the other hand, from Fig. 8 it follows that for the period of slightly increased local seismic activity in October 2010, the distribution of scaling exponents resembles the pattern observed in the period when the strong *M*6.0 Racha earthquake occurred. In this case, the scaling exponents' values calculated for ambient noise remain characteristic for correlated process, though they are shifted to the left, closer to $\alpha = 1.5$.

Next, though we have used DFA for ambient noises data, we additionally investigated increments' time series of original time series in order to further exclude a possible influence of different kinds of trends.

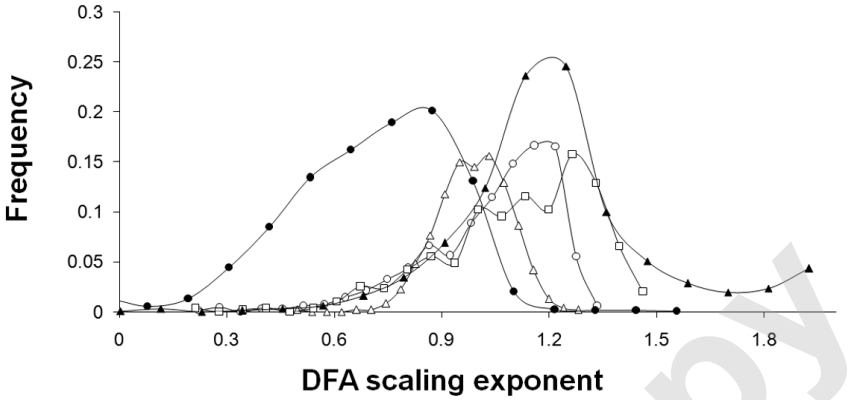

Fig. 9. The histograms of scaling exponents calculated for increment time series of noise *Z*-components data sets recorded at the Oni station. Calculation have been carried out for consecutive 12 000 sample data length windows of increment data sets for the periods regarded as seismically calm. Description of symbols as in Fig. 8.

In Figure 9 we see that scaling exponents of differenced data (increments' time series) are shifted to the left comparing to the results in Fig. 8. It is quite logical that the differentiation of ambient noise time series decreases their scaling exponent (in the histogram we see a decrease by about one). Most importantly, the distribution functions of scaling exponents of increments of ambient noise data are still different for time periods of increased and decreased local seismic activity around the Oni station (dark circles and triangles in Fig. 9). Moreover, disposition to the each other of the scaling exponents distribution curves, calculated for data recorded at other calm and/or activated seismic conditions, is similar to that presented in Fig. 8. This points out that the obtained results concerning features of distribution of scaling exponents at different local seismic conditions are not influenced by different possible trends.

Next, knowing that the ambient noises may be caused by a diversity of different, often unrelated and continuous sources of diverse origins from spatially distributed local and remote sources (SESAME 2004), we carried out an analysis in different frequency ranges, similar to the above analysis. We started from frequency interval of 0.04-4 Hz to cover the whole microseism activity range (Webb 1998). Specifically, we filtered original data to analyze scaling features of ambient noises for the following frequency contents: (i) below a frequency of 0.04 Hz, (ii) in the frequency range of 0.04 to 4 Hz, and (iii) above 4 Hz. By this, we aimed to clear up which frequency band of ambient noise is responsible for the changes observed in fluctuation scaling features.

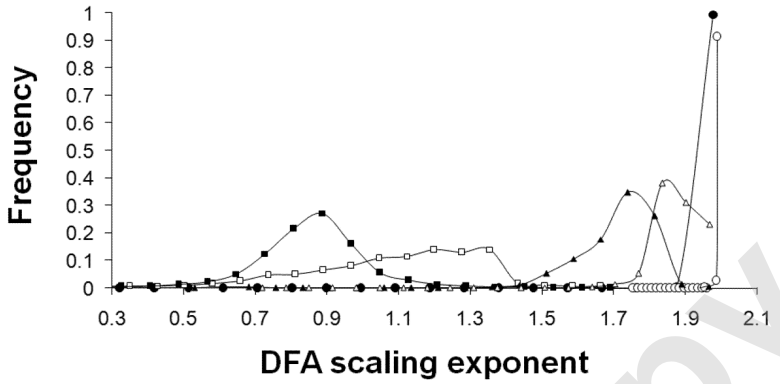

Fig. 10. The histograms of scaling exponents calculated for different frequency bands of ambient noise data sets. Prior to the Oni *M*6.0 (black symbols), before arrival of waveforms from the Japan *M*9.0 EQ (white symbols). For the frequencies: below 0.04 Hz (squares), in the range of 0.04-4 Hz (triangles), and above 4 Hz (circles).

We see in Fig. 10 that the high frequency range, above 4 Hz, which is regarded as caused by local and cultural noises (Webb 1998, SESAME 2004), does not reveal changes during the considered periods in September 2009 and March 2011. This is quite logical because the location of station or industrial or ambient conditions in the small town of Oni have not changed. In the low frequency range, below 0.04 Hz, where the influence of infragravity oceanic waves is predominant, we see clear difference between ambient noise scaling exponent distributions. It is very difficult to comment now but still worth to mention that before and after the Oni 6.0 earthquake that occurred in September 2009, low frequency ambient noises showed predominantly persistent behavior; the calculated DFA scaling exponent values (about 70%) are in 0.7-0.9 range. In the locally quiet period of March 2011 broad diversity of behaviours, from random to Brownian motion, was observed ($0.5 < \alpha < 1.5$). Most important for the purpose of the present paper is that such a difference is opposite to what we observe in original data as well as in filtered data in the 0.04-4 Hz frequency range. From these results we can conclude that differences found between fluctuation features of ambient noises at activated and calm local seismicity conditions, apparently cannot be caused by high or low frequency components and should be related to microseisms' constituents.

Results of similar analysis for calm time intervals selected from the above-mentioned periods in September 2009 and March 2011 provide additional arguments for such a conclusion. Indeed, in Fig. 11 we see that the distribution of scaling exponents for high and low frequency ranges are akin

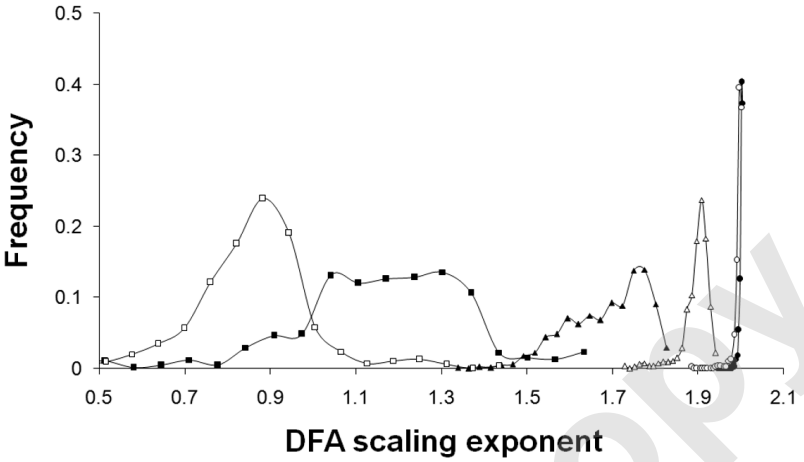

Fig. 11. The histograms of scaling exponents calculated for different frequency bands of ambient noise data sets compiled for calm periods, when no local earthquakes or arrival of waveforms from remote seismic activity were detected at the Oni station. Prior to the Oni *M*6.0 EQ (black symbols), before arrival of waveforms from the Japan *M*9.0 EQ (white symbols). For frequencies below 0.04 Hz (squares), in the range of 0.04-4 Hz (triangles), and above 4 Hz (circles).

to those shown in Fig. 10 for the whole time series. At the same time, in microseisms' frequency range of 0.04-4 Hz, the difference between distribution features of ambient noises scaling exponents in time period before the Oni *M*6.0 earthquake are clearly different from those in locally quiet period in March 2009, prior and after the arrival of wavetrains from the Japan *M*9.0 earthquake.

Afterwords, we decided to focus on the fluctuation features in the frequency bands directly contributing to the observed linear scaling parts of $\log F(n)$ *versus* $\log n$ curves of the considered ambient noise data. Specifically, from the analysis of fluctuation curves in Figs. 4 and 7 it follows that, in average, the scaling holds for time scales between crossovers at about 0.3 and 3 s (upper curves) and 0.2 and 3 s (lower curves). Therefore, we have filtered our data to analyze ambient noise scaling features in the frequency range of 0.3-3.8 Hz for the period when strong local earthquakes occurred in September 2009 and in the frequency range of 0.3-5 Hz for the period when wavetrains from the remote Japan earthquake arrived in March 2011. The results of analysis are presented in Fig. 12. As it follows from a comparison of this figure and previous ones (Figs. 10 and 11), the shift of high frequency threshold (from 4 to 3.8 Hz for activated and from 4 to 5 Hz for calm seismic conditions) of the considered ambient noise data has almost no effect on the distribution of scaling exponent values. The ambient noise

still looks like a persistent process for the period of activated local seismicity (white squares) and indicates wide distribution features for calm seismic conditions. Contrary to this, slight change in low frequency threshold, from 0.04 to 0.3 Hz, in the considered ambient noise data led to the noticeable change in observed fluctuation features (compare black and white circles in Figs. 10 and 12). It is worth mentioning that at calm conditions of local seismicity, the scaling exponents' values range is wider than for period of active seismicity. The most important fact is that neither low nor high frequency components of considered ambient noises do show any scaling features which could have masked differences observed in targeted frequency intervals, of 0.3-3.8 Hz for the time period when strong local earthquakes occurred in September 2009 and in the range of 0.3-5 Hz for the time period when wavetrains from the remote Japan earthquake arrived at Oni station in March 2011. Thus, it can be suggested that the observed differences in dynamics of ambient noises revealed through the differences in the fluctuation scaling exponents are related to processes directly contributing to local earthquake preparation.

As it was said above, prior to the strong local Oni *M*6.0 earthquake the values of DFA scaling exponents are distributed in a wide range, indicating coincidence of different dynamical behaviors with a slight dominance of long-range persistent correlations in ambient noises.

The origin of the shift from mostly persistent long-range correlated pattern in calm periods to the mixture of different fluctuation patterns, including antipersistent correlated and uncorrelated behavior at increased

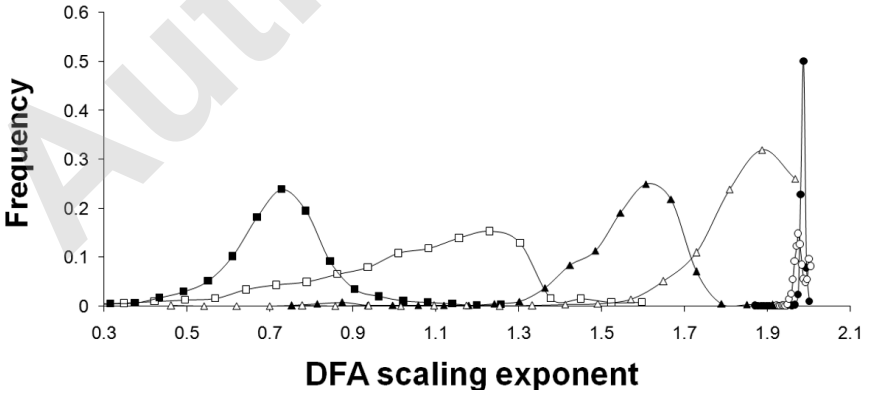

Fig. 12. The histograms of the scaling exponents calculated for different frequency bands of ambient noise data sets. Time period in September 2009: below 0.3 Hz (black squares), 0.3-3.8 Hz (black triangles), and above 3.8 Hz (black circles). Time period in March 2011: below 0.3 Hz (white squares), 0.3-5 Hz (white triangles), and above 5 Hz (white circles).

local seismic activity, remains mostly unclear, though it may be speculated that it is related to the distortion of dynamical structure of the background Earth surface vibration pattern under the influence of earthquake preparation processes.

The findings that fractal dimensions of ambient noise and seismic signals may be different, and that the probability density function (PDF) of ambient noise may undergo a transition from Gaussian to long-tailed non-Gaussian distribution prior to moderate and large earthquakes (Padhy 2004, Tabar *et al.* 2006, Manshour *et al.* 2009, 2010) are, from general point of view, in agreement with our results.

4. CONCLUSIONS

On the example of seismic noise data sets recorded at the Oni seismic station we have shown that, generally speaking, the ambient noise data sets are, for a wide time scale, characterized by long range persistent correlations.

Fluctuation properties of ambient noise are significantly affected by an influence of seismic waves from both local and remote earthquakes. At the same time, wavetrains from remote events cause quantitative changes in ambient noise data scaling properties, while seismic waves from local earthquakes lead to their complete qualitative distortions.

The analysis carried out on data sets from the epicentral zone of Oni M6.0 earthquake supports the opinion that scaling properties of ambient noise prior to strong local earthquakes may be quantifiable. The increased seismic activity can be accompanied by a distortion of persistent long-range correlations and an appearance of mixture of dynamical constituents with diverse persistent, antipersistent, and random behaviors.

References

Alvarez-Ramirez, J., G. Espinosa-Paredes, and A. Vazquez (2005), Detrended fluctuation analysis of the neutronic power from a nuclear reactor, *Physica A* **351**, 2-4, 227-240, DOI: 10.1016/j.physa.2004.08.087.

Bunde, A., J. Kropp, and H.J. Schellnhuber (eds.) (2002), *The Science of Disasters: Climate Disruptions, Heart Attacks, and Market Crashes*, Springer, Berlin.

Caserta, A., G. Consolini, and P. De Michelis (2007), Statistical features of the seismic noise-field, *Stud. Geophys. Geod.* **51**, 2, 255-266, DOI: 10.1007/s11200-007-0013-8.

Chelidze, T., and T. Matcharashvili (2007), Complexity of seismic process; measuring and applications – A review, *Tectonophysics* **431**, 1-4, 49-60, DOI: 10.1016/j.tecto.2006.05.029.

Chelidze, T., O. Lursmanashvili, T. Matcharashvili, and M. Devidze (2006), Triggering and synchronization of stick slip: Waiting times and frequency-energy distribution, *Tectonophysics* **424**, 3-4, 139-155, DOI: 10.1016/ j.tecto.2006.03.031.

Correig, A.M., M. Urquizu, J. Vila, and R. Macià (2007), Microseism activity and equilibrium fluctuations. **In**: A. Tsonis and J. Elsner (eds.), *Nonlinear Dynamics in Geosciences*, Springer, Berlin, 69-85, DOI: 10.1007/978-0-387-34918-3_5.

Goltz, C. (1997), Fractal and chaotic properties of earthquakes, *Lect. Notes Earth Sci*. **77**, 3-164, DOI: 10.1007/BFb0028315.

Hu, K., P.Ch. Ivanov, Z. Chen, P. Carpena, and H.E. Stanley (2001), Effect of trends on detrended fluctuation analysis, *Phys. Rev. E* **64**, 1, 011114, DOI: 10.1103/PhysRevE.64.011114.

Ivanov, P.Ch., A.L. Goldberger, and H.E. Stanley (2002), Fractal and multifractal approaches in physiology. **In**: A. Bunde, J. Kropp, and H.J. Schellnhuber (eds.), *The Science of Disasters: Climate Disruptions, Heart Attacks, and Market Crashes*, Springer-Verlag, Berlin, 219-257.

Kanamori, H., and E.E. Brodsky (2001), The physics of earthquakes, *Phys. Today* **54**, 6, 34-40, DOI: 10.1063/1.1387590.

Kantelhardt, J.W., S.A. Zschiegner, E. Koscielny-Bunde, S. Havlin, A. Bunde, and H.E. Stanley (2002), Multifractal detrended fluctuation analysis of nonstationary time series, *Physica A* **316**, 1-4, 87-114, DOI: 10.1016/ S0378-4371(02)01383-3.

Kapiris, P.G., K.A. Eftaxias, K.D. Nomikos, J. Polygiannakis, E. Dologlou, G.T. Balasis, N.G. Bogris, A.S. Peratzakis, and V.E. Hadjicontis (2003), Evolving towards a critical point: A possible electromagnetic way in which the critical regime is reached as the rupture approaches, *Nonlin. Processes Geophys.* **10**, 6, 511-524, DOI: 10.5194/npg-10-511-2003.

Karamanos, K., D. Dakopoulos, K. Aloupis, A. Peratzakis, L. Athanasopoulou, S. Nikolopoulos, P. Kapiris, and K. Eftaxias (2006), Preseismic electromagnetic signals in terms of complexity, *Phys. Rev. E* **74**, 1, 016104, DOI: 10.1103/PhysRevE.74.016104.

Keilis-Borok, V.I., and A.A. Soloviev (eds.) (2003), *Nonlinear Dynamics of the Lithosphere and Earthquake Prediction*, Springer-Verlag, Berlin.

Lapenna, V., M. Macchiato, and L. Telesca (1998), $1/f^{\beta}$ Fluctuations and self-similarity in earthquake dynamics: observational evidences in southern Italy, *Phys. Earth Planet. Inter*. **106**, 1-2, 115-127, DOI: 10.1016/S0031-9201(97)00080-0.

Lyubushin, A. (2010), Multifractal parameters of low-frequency microseisms. **In:** V. de Rubeis, Z. Czechowski, and R. Teisseyre (eds.), *Synchronization and Triggering: from Fracture to Earthquake Processess*, GeoPlanet: Earth and Planetary Sciences, Vol. 1, Springer-Verlag, Berlin, 253-272, DOI: 10.1007/ 978-3-642-12300-9_15.

Manshour, P., S. Saberi, M. Sahimi, J. Peinke, A.F. Pacheco, and M.R.R. Tabar (2009),Turbulencelike behavior of seismic time series, *Phys. Rev. Lett.* **102**, 1, 014101, DOI: 10.1103/PhysRevLett.102.014101.

Manshour, P., F. Ghasemi, T. Matsumoto, J. Gómez, M. Sahimi, J. Peinke, A.F. Pacheco, and M.R.R. Tabar (2010), Anomalous fluctuations of vertical velocity of Earth and their possible implications for earthquakes, *Phys. Rev. E* **82**, 3, 036105, DOI: 10.1103/PhysRevE.82.036105.

Matcharashvili, T., and T. Chelidze (2010), Nonlinear dynamics as a tool for revealing synchronization and ordering in geophysical time series: Application to caucasus seismicity. **In:** V. de Rubeis, Z. Czechowski, and R. Teisseyre (eds.), *Synchronization and Triggering: from Fracture to Earthquake Processess*, GeoPlanet: Earth and Planetary Sciences, Vol. 1, Springer, Berlin, 3-21, DOI: 10.1007/978-3-642-12300-9_1.

Matcharashvili, T., T. Chelidze, and Z. Javakhishvili (2000), Nonlinear analysis of magnitude and interevent time interval sequences for earthquakes of Caucasian region, *Nonlin. Processes Geophys.* **7**, 1/2, 9-20, DOI: 10.5194/npg-7-9-2000.

Padhy, S. (2004), Rescaled range fractal analysis of a seismogram for identification of signals from an earthquake, *Curr. Sci.* **87**, 5, 637-641.

Peng, C.-K., S.V. Buldyrev, A.L. Goldberger, S. Havlin, M. Simons, and H.E. Stanley (1993a), Finite-size effects on long-range correlations: Implications for analyzing DNA sequences, *Phys. Rev. E* **47**, 5, 3730-3733, DOI: 10.1103/PhysRevE.47.3730.

Peng, C.-K., J. Mietus, J. Hausdorff, S. Havlin, H.E. Stanley, and A.L. Goldberger (1993b), Long-range anticorrelations and non-Gaussian behavior of the heartbeat, *Phys. Rev. Lett.* **70**, 9, 1343-1346, DOI: 10.1103/PhysRevLett. 70.1343.

Peng, C.-K., S. Havlin, H.E. Stanley, and A.L. Goldberger (1995), Quantification of scaling exponents and crossover phenomena in nonstationary heartbeat time series, *Chaos* **5**, 1, 82-87, DOI: 10.1063/1.166141.

Rodriguez, E., J.C. Echeverria, and J. Alvarez-Ramirez (2007), Detrended fluctuation analysis of heart intrabeat dynamics, *Physica A* **384**, 2, 429-438, DOI: 10.1016/j.physa.2007.05.022.

Rundle, J.B., D.L. Turcotte, and W. Klein (eds.) (2000), *GeoComplexity and the Physics of Earthquakes*, AGU Monograph 120, American Geophysical Union, Washington, DC, 284 pp.

Ryabov, V.B., A.M. Correig, M. Urquizú, and A.A. Zaikin (2003), Microseism oscillations: from deterministic to noise-driven models, *Chaos Soliton. Fract.* **16**, 2, 195-210, DOI: 10.1016/S0960-0779(02)00165-0.

Scholz, C.H. (1990), *The Mechanics of Earthquakes and Faulting*, Cambridge University Press, Cambridge.

SESAME (2004), Guidelines for the implementation of the H/V spectral ratio technique on ambient vibrations. Measurements, processing and interpretation,

WP12 European Commission – Research General Directorate, Project No. EVG1-CT-2000-0026 SESAME, report D23.

Sobolev, G.A., and A.A. Lyubushin (2006), Microseismic impulses as earthquake precursors, *Izv. – Phys. Solid Earth* **42**, 9, 721-733, DOI: 10.1134/S1069351306090023.

Sobolev, G.A., A.A. Lyubushin, and N.A. Zakrzhevskaya (2010), Synchronizations of microseismic oscillations as the indicators of the instability of a seismically active region. **In:** V. de Rubeis, Z. Czechowski, and R. Teisseyre (eds.), *Synchronization and Triggering: from Fracture to Earthquake Processess*, GeoPlanet: Earth and Planetary Sciences, Vol. 1, Springer, Berlin, 243-252, DOI: 10.1007/978-3-642-12300-9_14.

Tabar, M.R.R., M. Sahimi, F. Ghasemi, K. Kaviani, M. Allamehzadeh, J. Peinke, M. Mokhtari, M. Vesaghi, M.D. Niry, A. Bahraminasab, S. Tabatabai, S. Fayazbakhsh, and M. Akbari (2006), Short-term prediction of medium- and large-size earthquakes based on Markov and extended self-similarity analysis of seismic data, *Lect. Notes Phys.* **705**, 281-301, DOI: 10.1007/3-540-35375-5_11.

Telesca, L., and V. Lapenna (2006), Measuring multifractality in seismic sequences, *Tectonophysics* **423**, 1-4, 115-123, DOI: 10.1016/j.tecto.2006.03.023.

Telesca, L., V. Lapenna, and M. Macchiato (2005), Multifractal fluctuations in seismic interspike series, *Physica A* **354**, 629-640, DOI: 10.1016/j.physa.2005.02.053.

Telesca, L., M. Lovallo, V. Lapenna, and M. Macchiato (2008), Space-magnitude dependent scaling behaviour in seismic interevent series revealed by detrended fluctuation analysis, *Physica A* **387**, 14, 3655-3659, DOI: 10.1016/j.physa.2008.02.035.

Theiler, J., S. Eubank, A. Longtin, B. Galdrikian, and J.D. Farmer (1992), Testing for nonlinearity in time series: the method of surrogate data, *Physica D* **58**, 1-4, 77-94, DOI: 10.1016/0167-2789(92)90102-S.

Webb, S.C. (1998), Broadband seismology and noise under the ocean, *Rev. Geophys*. **36**, 1, 105-142, DOI: 10.1029/97RG02287.

Yulmetyev, R., F. Gafarov, P. Hänggi, R. Nigmatullin, and S. Kayumov (2001), Possibility between earthquake and explosion seismogram differentiation by discrete stochastic non-Markov processes and local Hurst exponent analysis, *Phys. Rev. E* **64**, 6, 066132, DOI: 10.1103/PhysRevE.64.066132.

Yulmetyev, R., P. Hänggi, F. Gafarov, and D.G. Yulmetyeva (2003), Non-stationary time correlation in discrete complex systems: Applications in cardiology and seismology, *Nonlin. Phen. Compl. Systems* **6**, 3, 791-799.

Received 16 September 2011
Received in revised form 26 January 2012
Accepted 2 February 2012